A more detailed and quantitative consideration of organized convection: Part I

Cold pool dynamics and the formation of squall lines

Note: Lecture notes presented here based on course Daily Weather Laboratory II taught by Prof. Richard Johnson, Colorado State University, Department of Atmospheric Science

Why does convection organize on the mesoscale?

Mesoscale organization is common when the low-level shear is moderate or greater. The shear provides ample moisture supply to promote extended growth of the convection. System propagation and/or upper-level shear encourages spreading of ice (anvil cloud) aloft. Both processes enable development to larger scales.

Rotunno et al. (1988)

Other factors

- *midlatitude baroclinic systems*
- *convergence lines*
  - gust fronts (outflow boundaries)
  - drylines
  - sea/land breezes
- *gravity waves*
- *upper-level jet streaks*
- *low-level jets*
- *topographic effects*
- *others*

(e.g., boundary-layer circulations)

Rotunno, Klemp, and Wilhelmson (RKW) Theory: The visual picture

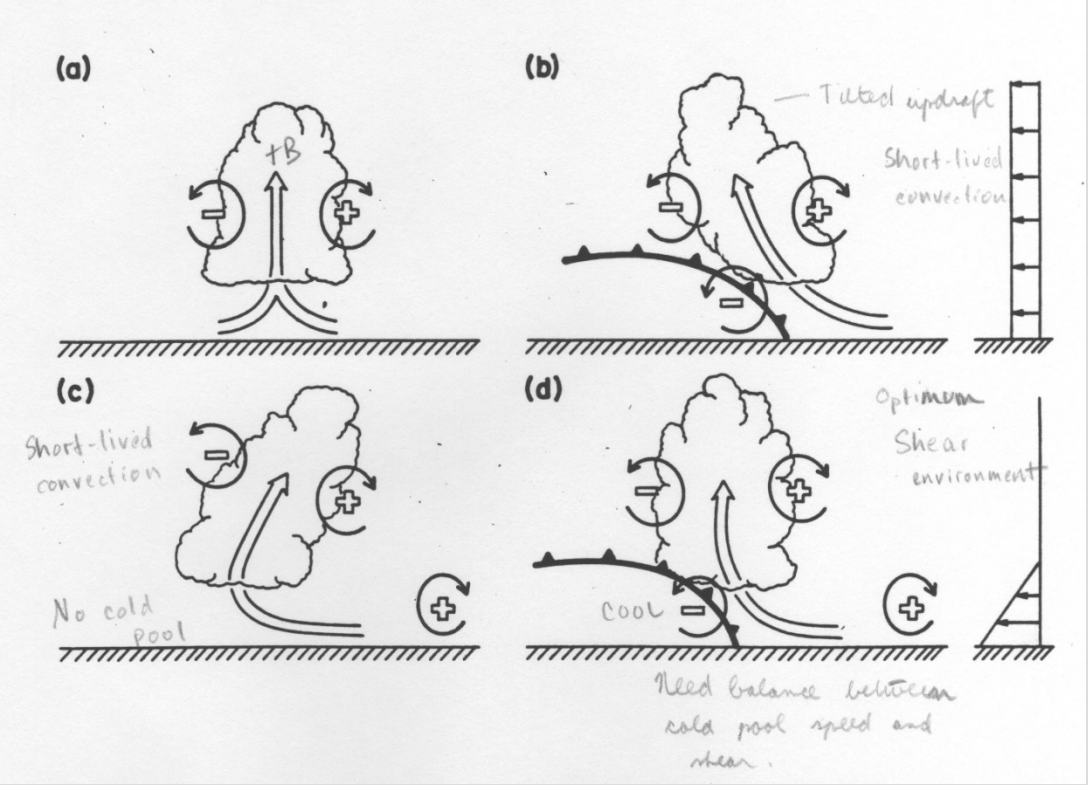

Schematic diagram showing how a buoyant updraft may be influenced by wind shear and/or a cold pool. (a) With no shear and no cold pool, the axis of the updraft produced by the thermally created, symmetric vorticity distribution is vertical. (b) With a cold pool, the distribution is biased by the negative vorticity of the underlying cold pool and causes the updraft to lean upshear. (c) With shear, the distribution is biased toward positive vorticity and this causes the updraft to lean back over the cold pool. (d) With both a cold pool and shear, the two effects may negate each other, and allow an erect updraft. (From Rotunno et al., 1988)

Mesovortices typically develop within mature-to-decaying MCSs. However, so far we have not examined the factors that determine the longevity of MCSs or squall lines. This issue has been studied by Rotunno et al. (1988) [hereafter referred to as RKW], among others. They consider the dynamics of squall lines in terms of the generation of vorticity η about a horizontal axis perpendicular to the squall line by horizontal buoyancy gradients. Referring to the vorticity fields illustrated in Fig. 20, with the x-direction to the right, the vorticity equation is

$$\frac{d\eta}{dt} = -\frac{\partial B}{\partial x} , \tag{7.14}$$

where

$$\eta \equiv \frac{\partial u}{\partial z} - \frac{\partial w}{\partial x} ,$$

Vorticity from wind components in x-z plane

and B = total buoyancy $= g\theta_v'/\bar{\theta}_v$. Using mass continuity,

$$\frac{\partial u}{\partial x} + \frac{\partial w}{\partial z} = 0 ,$$

(7.14) becomes

$$\frac{\partial \eta}{\partial t} = -\frac{\partial}{\partial x} u\eta - \frac{\partial}{\partial z} w\eta - \frac{\partial B}{\partial x} . \tag{7.15}$$

Expand total derivative

Consider the cold pool illustrated below:

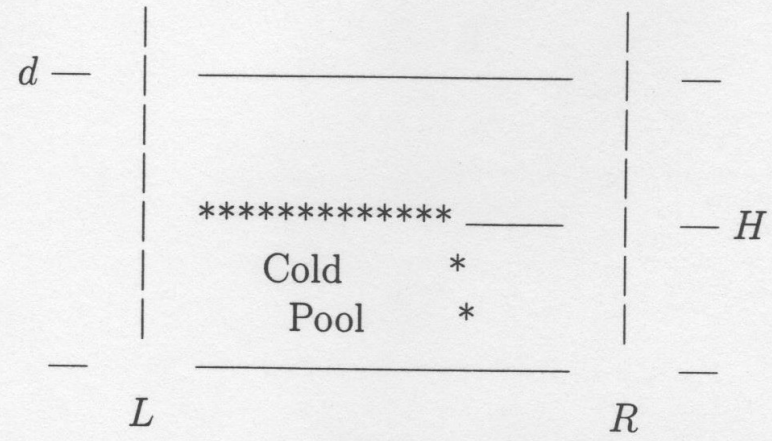

Cold pool on lower left side of the domain

We fix ourselves in a frame of reference moving with the edge of the cold air and integrate (7.15) from a point to the left, $x = L$, to a point to the right, $x = R$, of the cold-air edge, and from the ground to some level, $z = d$, and obtain

$$\underbrace{\frac{\partial}{\partial t}\int_L^R \int_0^d \eta \, dz \, dx}_{\text{tendency}} = \underbrace{\int_0^d (u\eta)_L dz}_{\text{flux at left}} - \underbrace{\int_0^d (u\eta)_R \, dz}_{\text{flux at right}}$$

$$- \underbrace{\int_L^R (w\eta)_d \, dx}_{\text{flux at top}} + \underbrace{\int_0^d (B_L - B_R) dz}_{\text{net generation}} . \qquad (7.16)$$

Vorticity tendency = Net advection of vorticity from sides + difference in buoyancy

Simplifying assumptions

Since we are looking for a steady balance, we set the tendency term to zero. Also, in the circumstances investigated by RKW, there is negligible buoyancy of the air approaching the cold pool, so $B_R = 0$. Finally, note that $\eta \approx \partial u/\partial z$ away from the edge of the cold air. Under these conditions, (7.16) becomes

$$0 = \left(\frac{u_{L,d}^2}{2} - \frac{u_{L,0}^2}{2}\right) - \left(\frac{u_{R,d}^2}{2} - \frac{u_{R,0}^2}{2}\right) - \int_L^R (w\eta)_d \, dx + \int_0^d B_L dz \, . \qquad (7.17)$$

Consider the situation where the cold air is stagnant (relative to the cold-air edge), so $u_{L,0} = 0$, and restricted to a height, $z = H$, where $H < d$. Thus,

$$0 = \frac{u_{L,d}^2}{2} - \left(\frac{u_{R,d}^2}{2} - \frac{u_{R,0}^2}{2}\right) - \int_L^R (w\eta)_d \, dx + \int_0^H B_L \, dz \, . \qquad (7.18)$$

Consider first the case where there is no shear at $x = R$ and a rigid plate at $z = d$. Under these conditions the second and third terms on the right-hand-side of (7.18) vanish and we obtain

$$u_{L,d}^2 = 2\int_0^H (-B_L) dz \equiv c^2$$

$$= 2g'H$$

where $-B_L = -g\Delta\theta/\theta_0 \equiv g'$ and the temperature deficit in the cold pool $\Delta\theta$ has been assumed constant. This reduces to the famous von Kármán formula for speed of gravity current as $d \to \infty$ since $u_{L,\infty} \to u_R$.

Vertical velocity zero at top

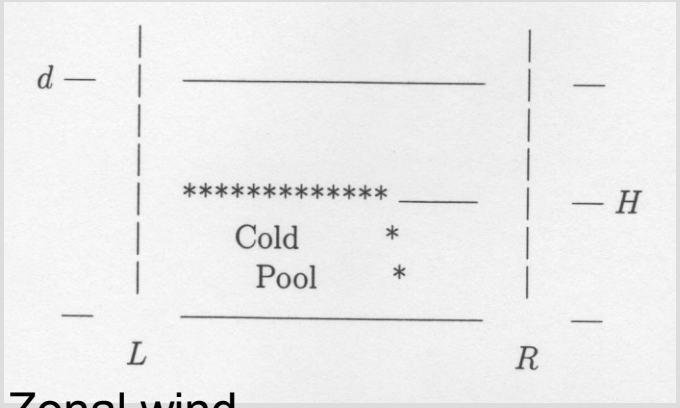

Zonal wind zero on lower left

No shear on right side (u=0)

Result: zonal wind at the upper boundary travels at the speed of a gravity current due to presence of the cold pool

Simplifying assumptions

Since we are looking for a steady balance, we set the tendency term to zero. Also, in the circumstances investigated by RKW, there is negligible buoyancy of the air approaching the cold pool, so $B_R = 0$. Finally, note that $\eta \approx \partial u/\partial z$ away from the edge of the cold air. Under these conditions, (7.16) becomes

$$0 = \left(\frac{u_{L,d}^2}{2} - \frac{u_{L,0}^2}{2}\right) - \left(\frac{u_{R,d}^2}{2} - \frac{u_{R,0}^2}{2}\right) - \int_L^R (w\eta)_d \, dx + \int_0^d B_L dz \, . \qquad (7.17)$$

Consider the situation where the cold air is stagnant (relative to the cold-air edge), so $u_{L,0} = 0$, and restricted to a height, $z = H$, where $H < d$. Thus,

$$0 = \frac{u_{L,d}^2}{2} - \left(\frac{u_{R,d}^2}{2} - \frac{u_{R,0}^2}{2}\right) - \int_L^R (w\eta)_d \, dx + \int_0^H B_L \, dz \, . \qquad (7.18)$$

Consider first the case where there is no shear at $x = R$ and a rigid plate at $z = d$. Under these conditions the second and third terms on the right-hand-side of (7.18) vanish and we obtain

$$u_{L,d}^2 = 2\int_0^H (-B_L) dz \equiv c^2$$

$$= 2g'H$$

where $-B_L = -g\Delta\theta/\theta_0 \equiv g'$ and the temperature deficit in the cold pool $\Delta\theta$ has been assumed constant. This reduces to the famous von Kármán formula for speed of gravity current as $d \to \infty$ since $u_{L,\infty} \to u_R$.

Vertical velocity zero at top

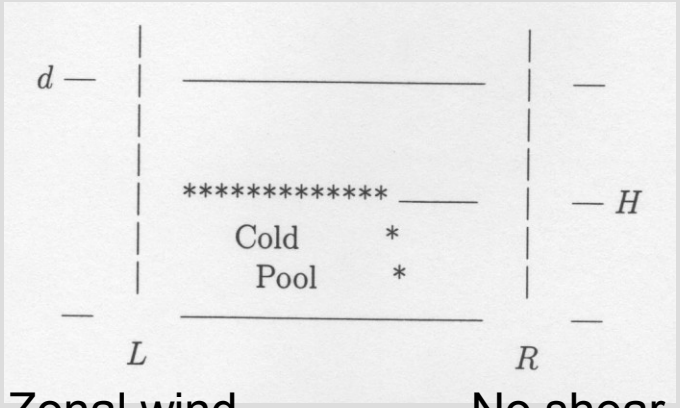

Zonal wind zero on lower left

No shear on right side

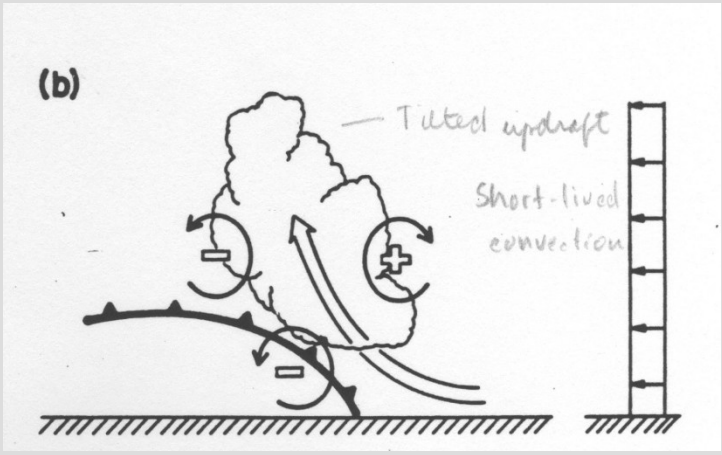

Result: zonal wind at the upper boundary travels at the speed of a gravity current due to presence of the cold pool

Consider now a case with low-level shear (Fig. 19d). Looking for an optimal state where the low-level flow is turned by the cold pool to exit vertically, we have

$$u_{L,d} = u_{R,d} = \int_L^R (w\eta)_d dx = 0$$

so

$$0 = +\frac{u_{R,0}^2}{2} + \int_0^H B_L dz$$

or

$$\Delta u = c\,, \qquad (7.19)$$

where $\Delta u = u_{R,d} - u_{R,0} = -u_{R,0}$ ($u_{R,0}$ is negative).

Equation (7.19) says that the import of positive vorticity associated with the low-level shear just balances the net buoyant generation of negative vorticity by the cold pool in the volume. The RKW hypothesis is then that the *strength and longevity of squall lines are maximized for this balance between the strength of the cold pool and the low-level shear* (a necessary, but not sufficient condition).

Vertical velocity zero at top

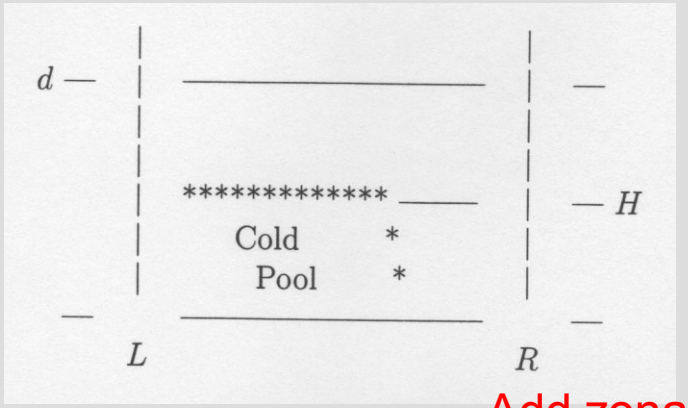

Zonal wind zero on lower left

Add zonal shear to this side

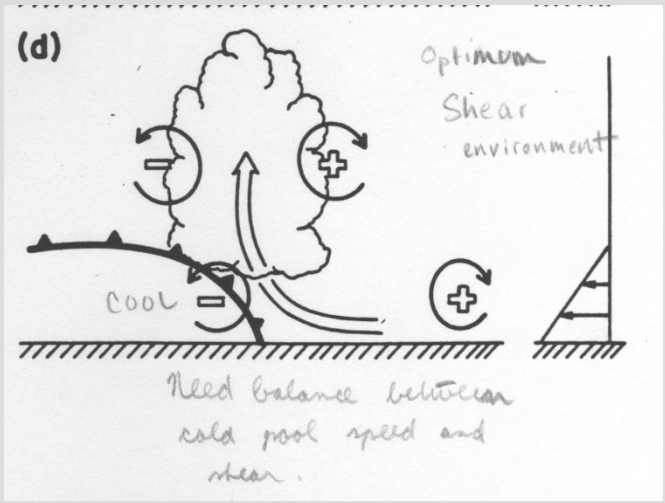

OPTIMAL CONVECTIVE STATE =
No inhibition of a vertically upright updraft by cold pool or shear.

Further development with the trailing stratiform region

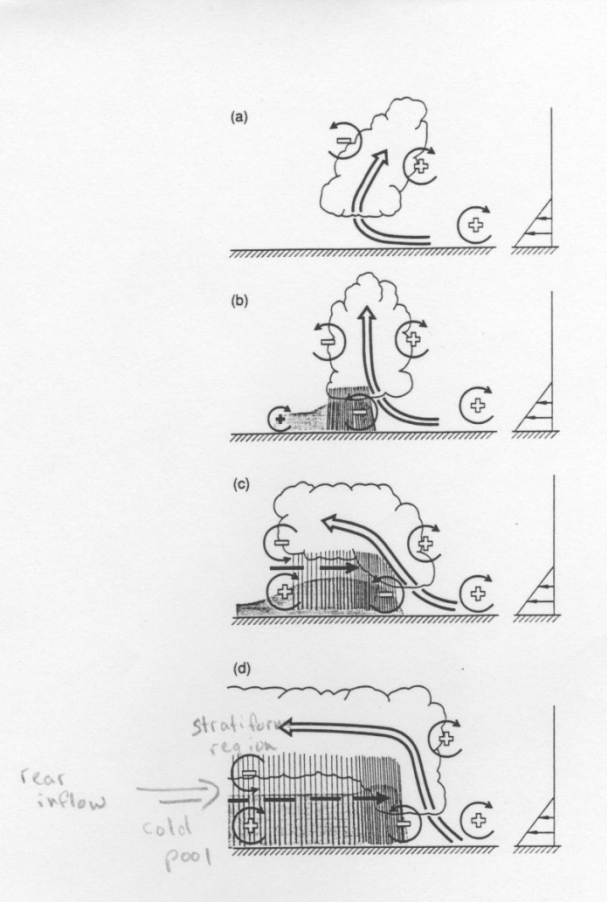

Four stages in the evolution of an idealized bow echo. (a) An initial updraft leans downshear in response to the ambient vertical wind shear, which is shown on the right. (b) The circulation generated by the storm-induced cold pool balances the ambient shear, and the system becomes upright. (c) The cold pool circulation overwhelms the ambient shear, and the system tilts upshear, producing a rear-infow jet. (d) A new steady state is achieved whereby the circulation of the cold pool is balanced by both the ambient vertical wind shear and the elevated rear-inflow jet. The updraft current is denoted by the thick double-lined flow vector, with the rear-inflow current in (c) and (d) denoted by the thick dashed vector. The shading denotes the surface cold pool. The thin, circular arrows depict the most significant sources of horizontal vorticity, which are either associated with the ambient shear or are generated within the convective system, as described in the text. Regions of lighter or heavier rainfall are indicated by the more sparsely or densely packed vertical lines, respectively. The scalloped line denotes the outline of the cloud (adapted from Weisman, 1992)

The upshear tilting of the updraft by a large cold pool causes the formation of a rear low level jet. This feature helps maintain the squall line, as it helps to oppose the cold pool horizontal vorticity.

Weakening squall line

Strengthening squall line

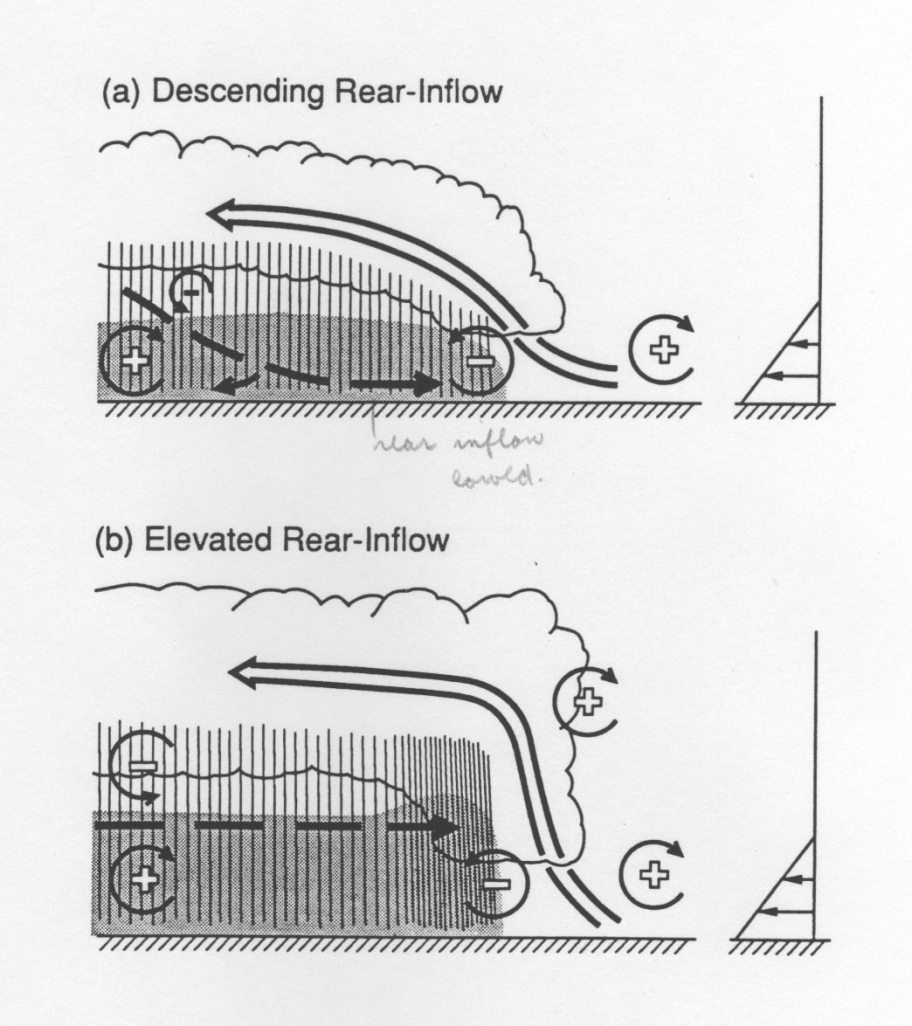

A conceptual model of the mature structure of a longlived squall-line-type convective system for (a) a system with a descending rear-inflow jet and (b) a system with an elevated rear-inflow jet. The updraft current is denoted by the thick, double-lined flow vector, while the rear-inflow current is denoted by the thick, dashed flow vector. The shading denotes the surface cold pool. The thin, circular arrows depict the most significant sources of horizontal vorticity, which are either associated with the ambient shear or which are generated within the convective system, as described in the text. Regions of lighter or heavier rainfall are indicated by the more sparsely or densely packed vertical lines, respectively. The scalloped line denotes the outline of the cloud. (From Weisman, 1992)

If the cold pool dynamics overwhelm the rear inflow jet, the squall line will tend to weaken.

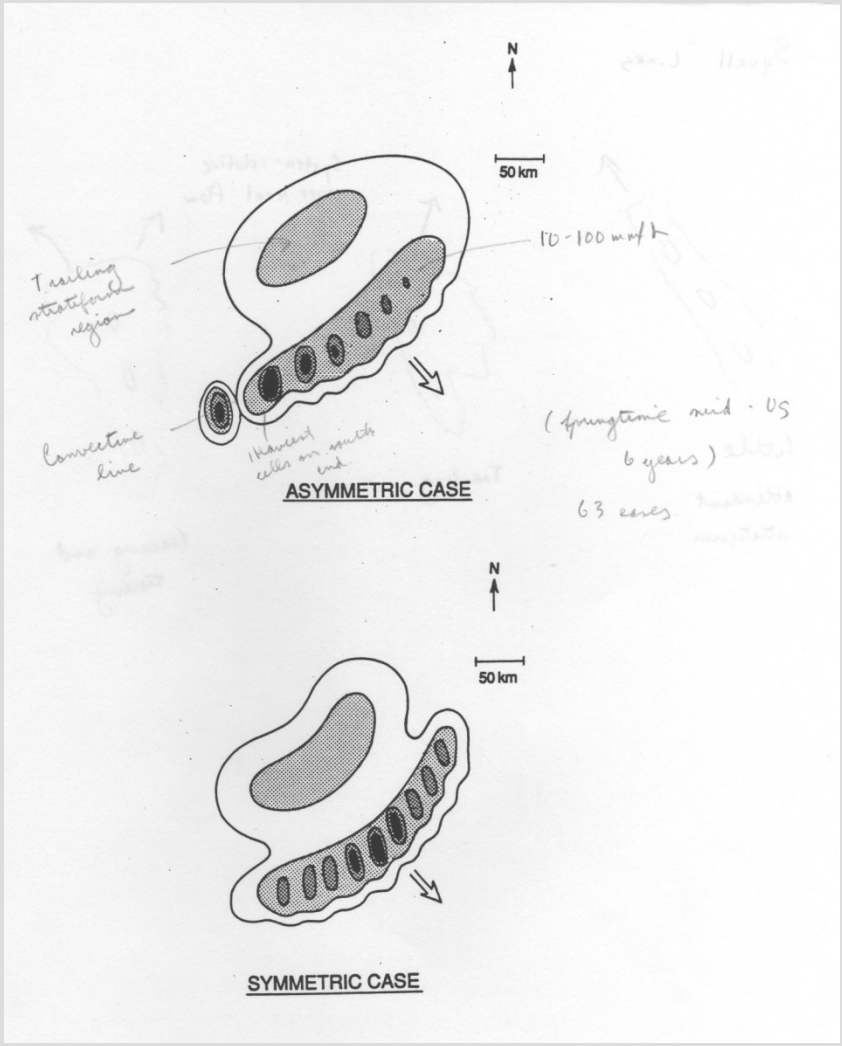

Schematic depicting Asymmetric (top) and Symmetric (bottom) pattern of leading line/trailing stratiform mesoscale precipitation system organization. Large vector indicates direction of system motion. Levels of shading denote increasing radar reflectivity, with most intense values corresponding to convective cell cores. (From Houze et al. 1990)

Asymmetric leading line

More common situation because of the influence of a varying Coriolis parameter. This will during the ascending inflow poleward and rear inflow jet equatorward.

Common in cold fronts since that the synoptic scale where varying f would matter more. Watch out for supercells at the end of the line (more on that later…)

Symmetric leading line

If the convection occurs more on the mesocale, can possibly be more symmetric in shape because variation in f is less important.

More common in mesoscale convective systems associated with bow echoes (derechos)

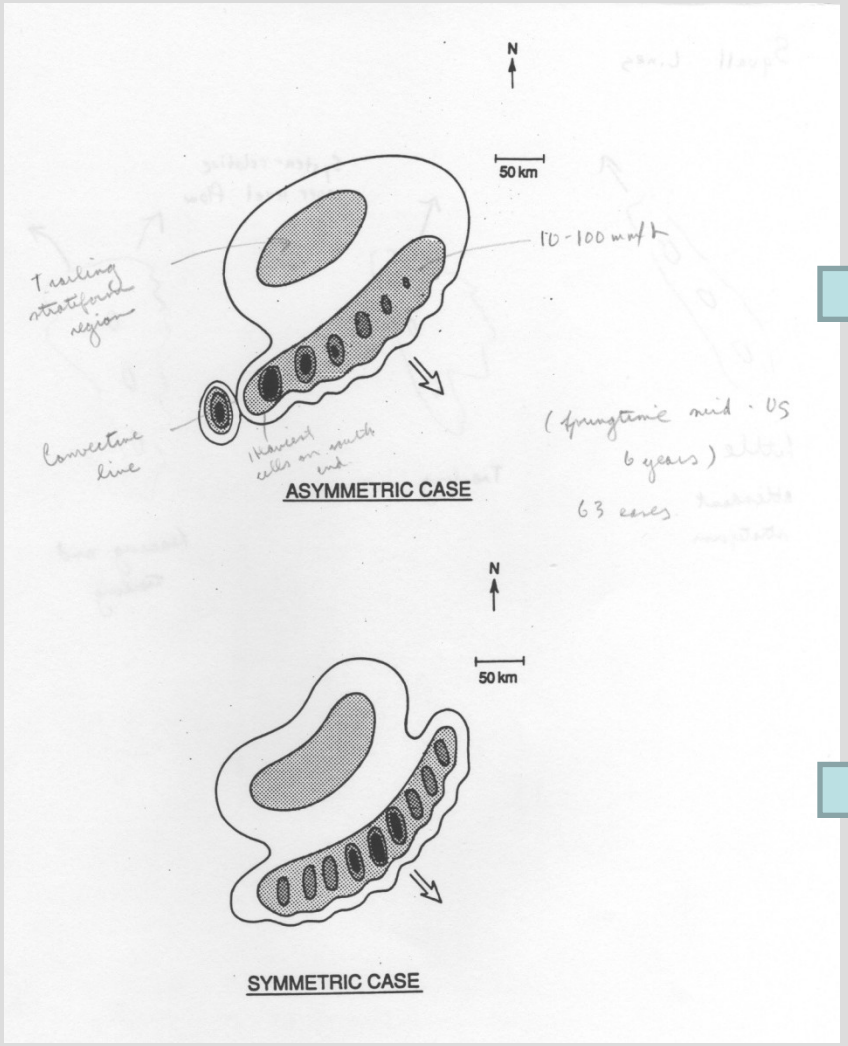

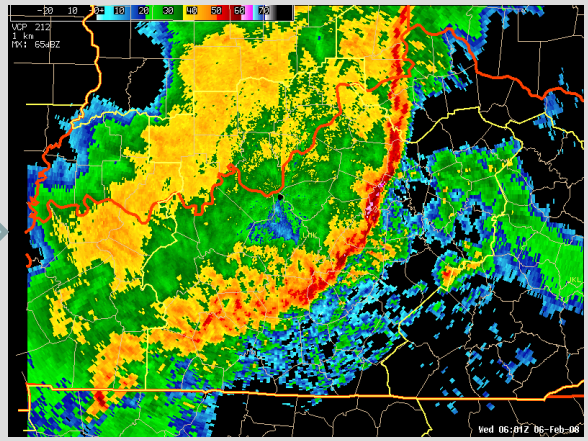

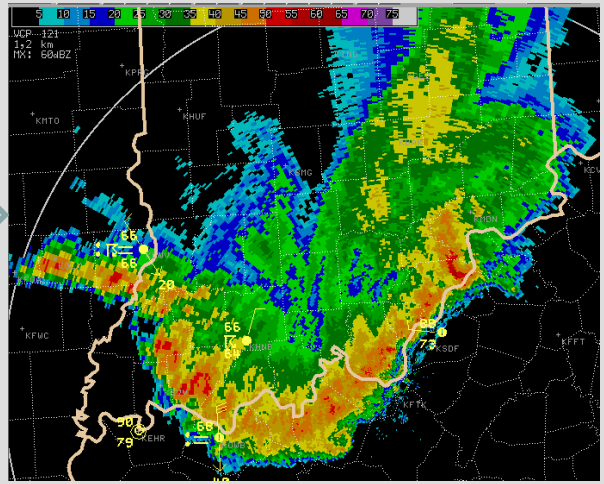

Schematic depicting Asymmetric (top) and Symmetric (bottom) pattern of leading line/trailing stratiform mesoscale precipitation system organization. Large vector indicates direction of system motion. Levels of shading denote increasing radar reflectivity, with most intense values corresponding to convective cell cores. (From Houze et al. 1990)

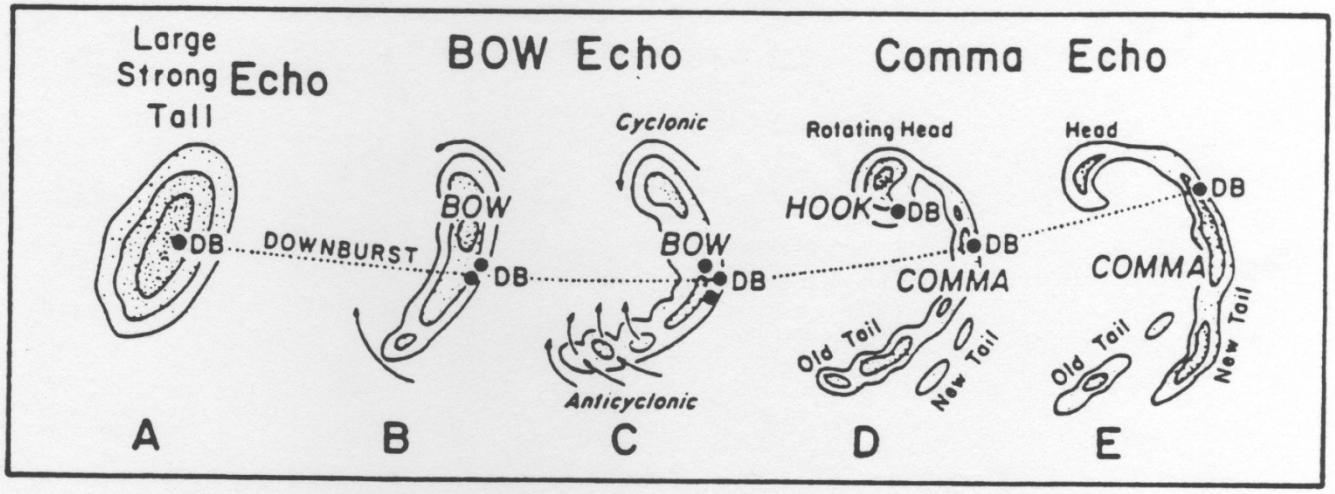

Fig. 14 A typical morphology of radar echoes associated with bow echoes that produce strong and extensive downbursts, labeled DB on the figure. (From Fujita 1978)

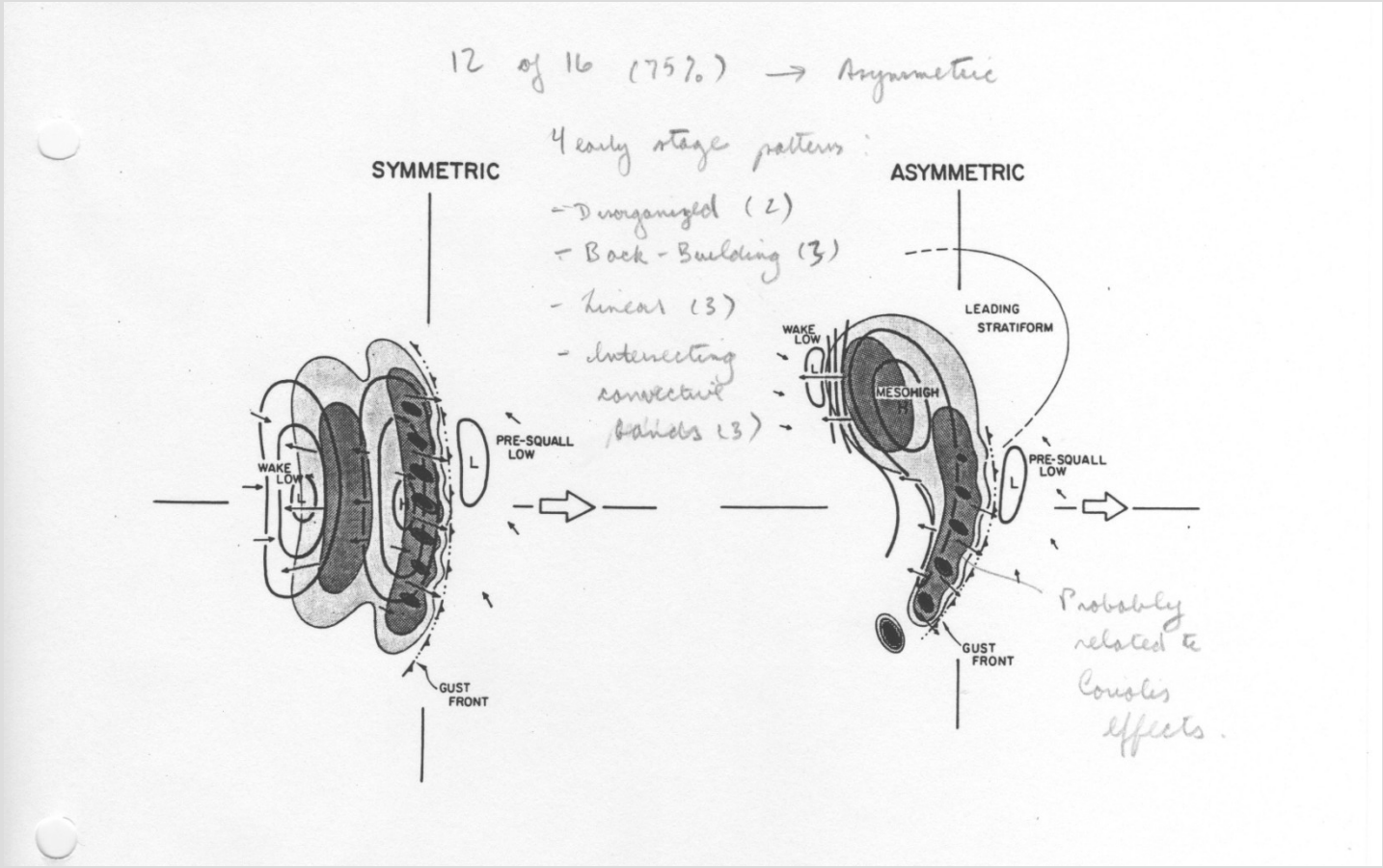

Schematic of surface pressure field (1-mb intervals) and ground-relative flow (arrows) associated with asymmetric (top) and symmetric (bottom) MCS precipitation patterns. Light and moderate shading represents radar reflectivities less than and greater than 30 dBZ, respectively. Heavy shading represents the convective line containing cells with reflectivities exceeding 40 dBZ. (From Loehrer and Johnson 1995)

Idealized simulation of symmetric squall lines with convective-resolving model

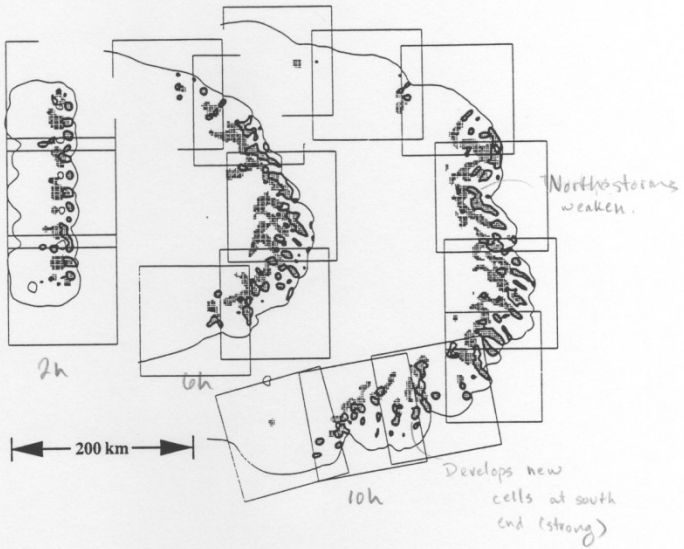

Horizontal cross sections form the Coriolis simulations at 3000 m plotted in ground-relative coordinates at 2, 6, and 10 h. Note the strong system growth and migration toward the southeast. The finest-resolution grids are included at the three times. (From Skamarock et al., 1994)

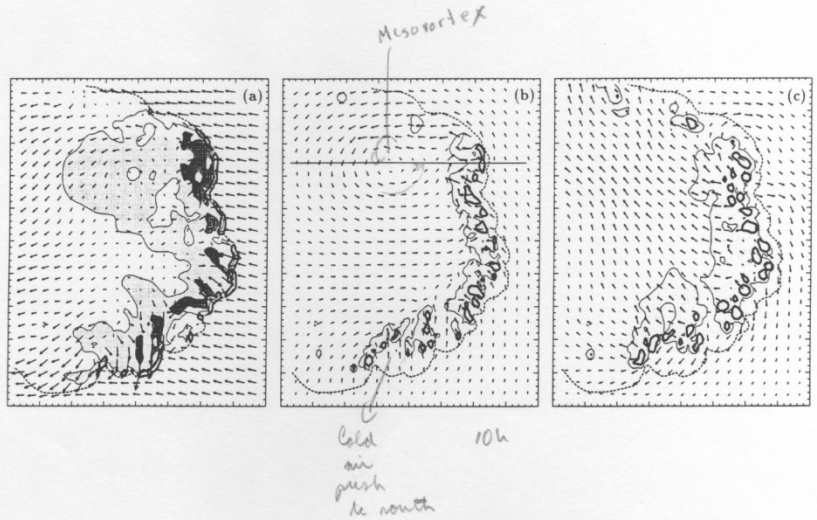

Fig. 19 The Coriolis simulation at 10 h. The flow vectors are storm relative with a system velocity $\bar{U} = 10$ m s^{-1} and where a vector length of one grid interval is 8 m s^{-1}. The plotting domain is 400 by 500 km. The dashed line represents the -1 K θ' contour and denotes the cold pool-gust front boundary, plotted at all levels for reference. At 350 m (a), the thick contour is $w > 0.5$ m s^{-1}. $\theta' <$ -4 K is highlighted by light stippling, and $\theta' <$ -6 K is highlighted by dark stippling. At 3000 m (b), $w > 2$ m s^{-1} is contoured and rainwater greater than 0.5 g kg^{-1} is stippled. At 8000 m (c), $w > 2$ m s^{-1} is contoured and cloud water greater than 0.1 g kg^{-1} is stippled. The data are plotted on a 6-km horizontal resolution grid. (From Skamarock et al., 1994)

A more detailed and quantitative consideration of organized convection: Part II

Mesoscale convective systems

Bob Maddox's classic MCS definition

	Physical characteristics
Size:	(A) Cloud shield with continuously low infrared temperature $\leq -32°C$ must have an area $\geq 100{,}000$ km^2 (B) Interior cold cloud region with temperature $\leq -52°C$ must have an area $\geq 50{,}000$ km^2
Initiate:	Size definitions (A) and (B) are first satisfied
Duration:	Size definitions (A) and (B) must be met for a period ≥ 6 hr
Maximum extent:	Contiguous cold cloud shield (infrared temperature $\leq -32°C$) reaches maximum size
Shape:	Eccentricity (minor axis/major axis) ≥ 0.7 at time of maximum extent
Terminate:	Size definitions (A) and (B) no longer satisfied

*From Maddox (1980)

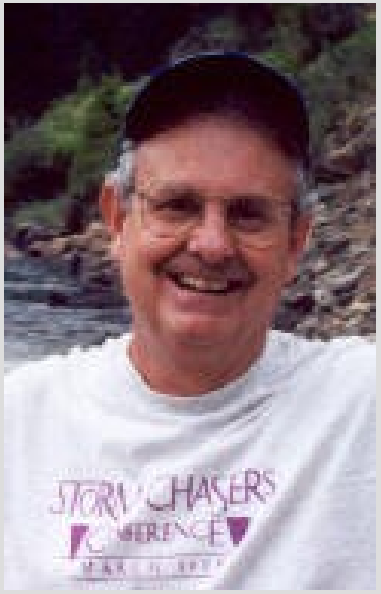

Climatological considerations for MCS development and maintenance

Downstream of mountain barriers (e.g. Rockies or Andes)

Vicinity of low-level jet, with strong low-level warm advection and deep moisture

For central US, form ahead of a weak, midlevel trough. Inverted trough if you are in the Southwest.

Maximum intensity usually occurs at night, when the low-level jet is strongest

Can modify the large-scale environment in a significant way

- Mesohighs and mesolows
- Mesoscale convective vortices (MCVs)

Unlike squall lines associated with mid-latitude cold fronts, MCS in the US tend to form around the periphery of an upper-level high in mid to late summer (when North American monsoon occurs). Strong monsoon convection in Arizona are typically caused by eastward propagating MCSs.

Ring of Fire Pattern on enhanced IR imagery: 22 July 2010

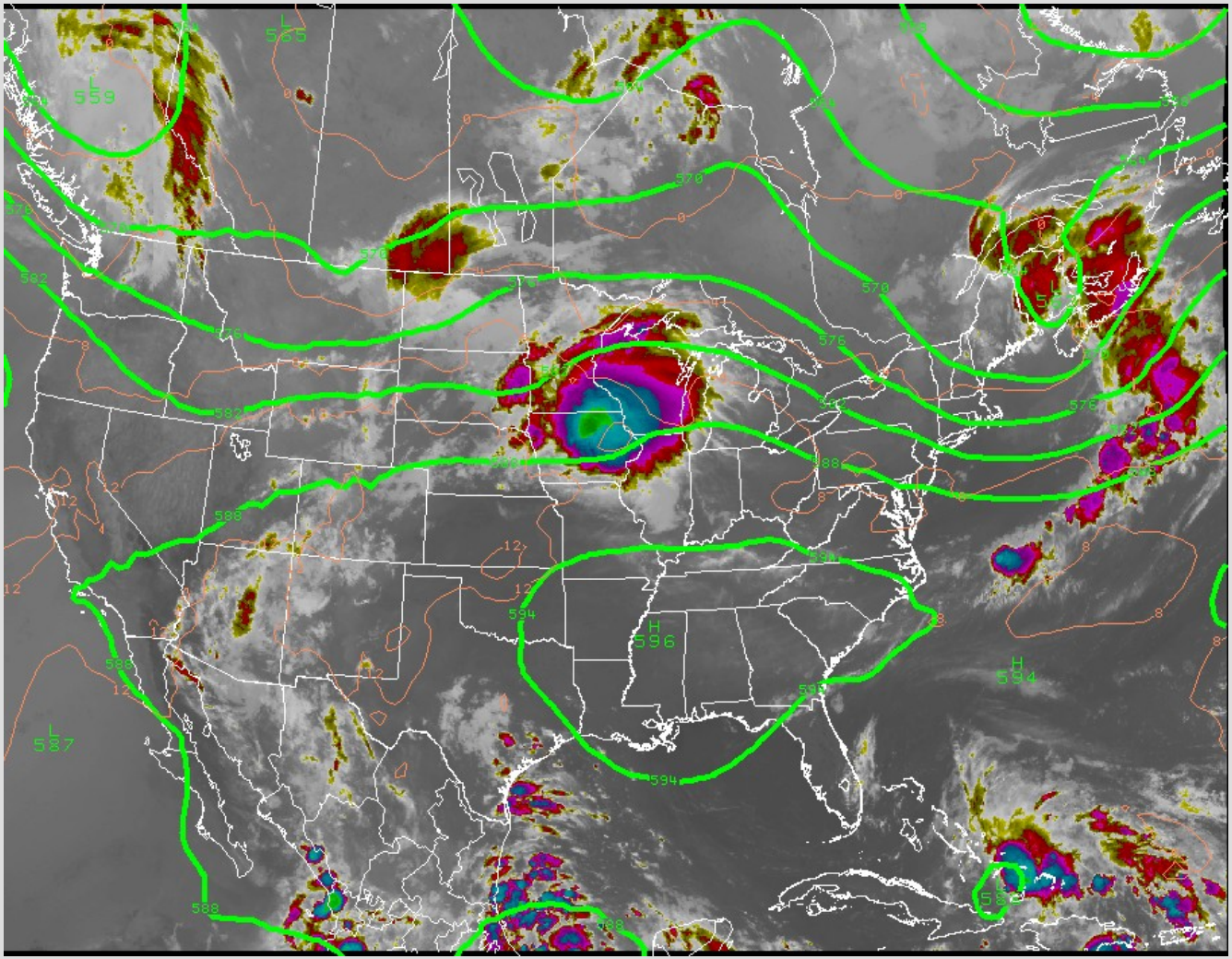

Climatology of MCSs in the Americas

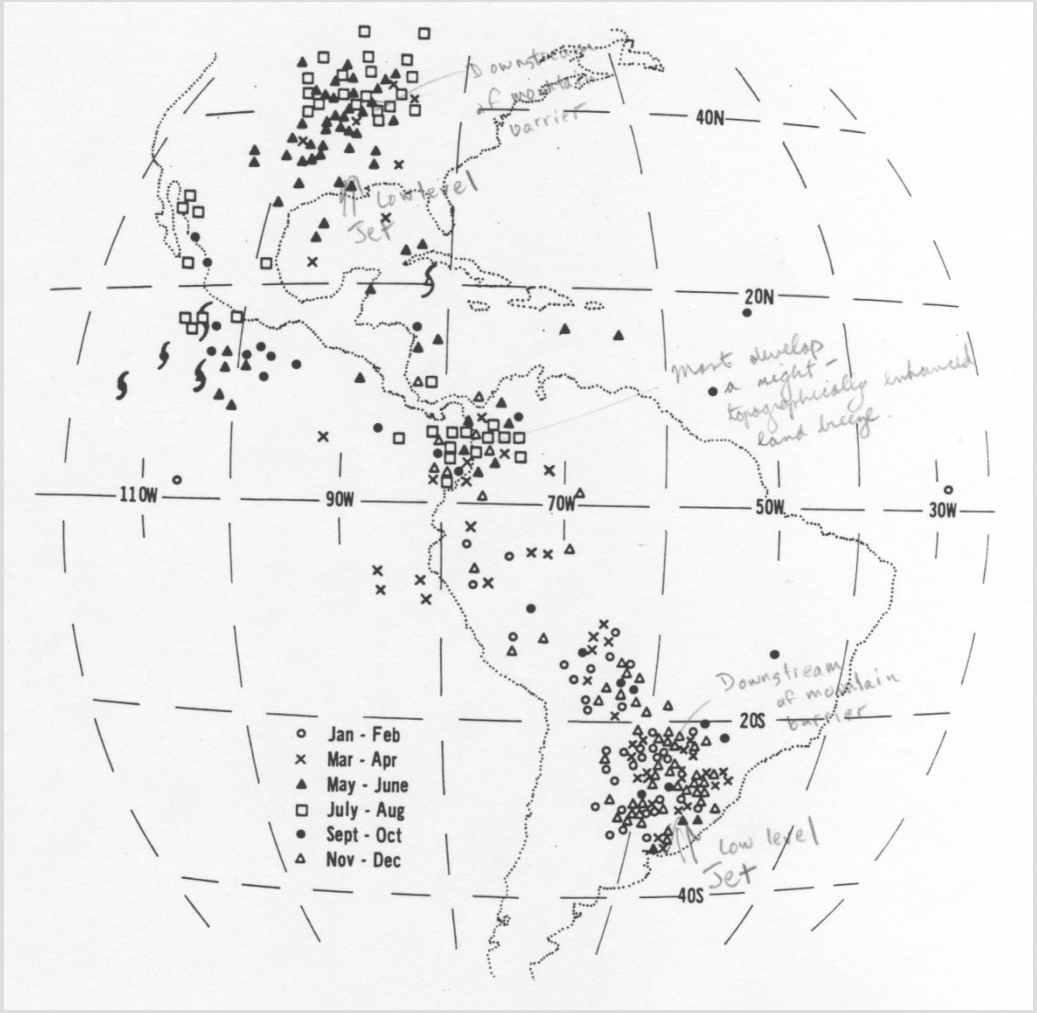

Geographic and monthly distribution of MCCs in and around the Americas. Locations are for the MCC cold-cloud shields at the time of maximum extent. See Velasco and Fritsch (1987) for sample periods. Hurricane symbols indicate an MCC that developed into a tropical storm. Systems that were first a tropical storm and then an MCC are not shown.

Idealized structure of a mature mesoscale convective system

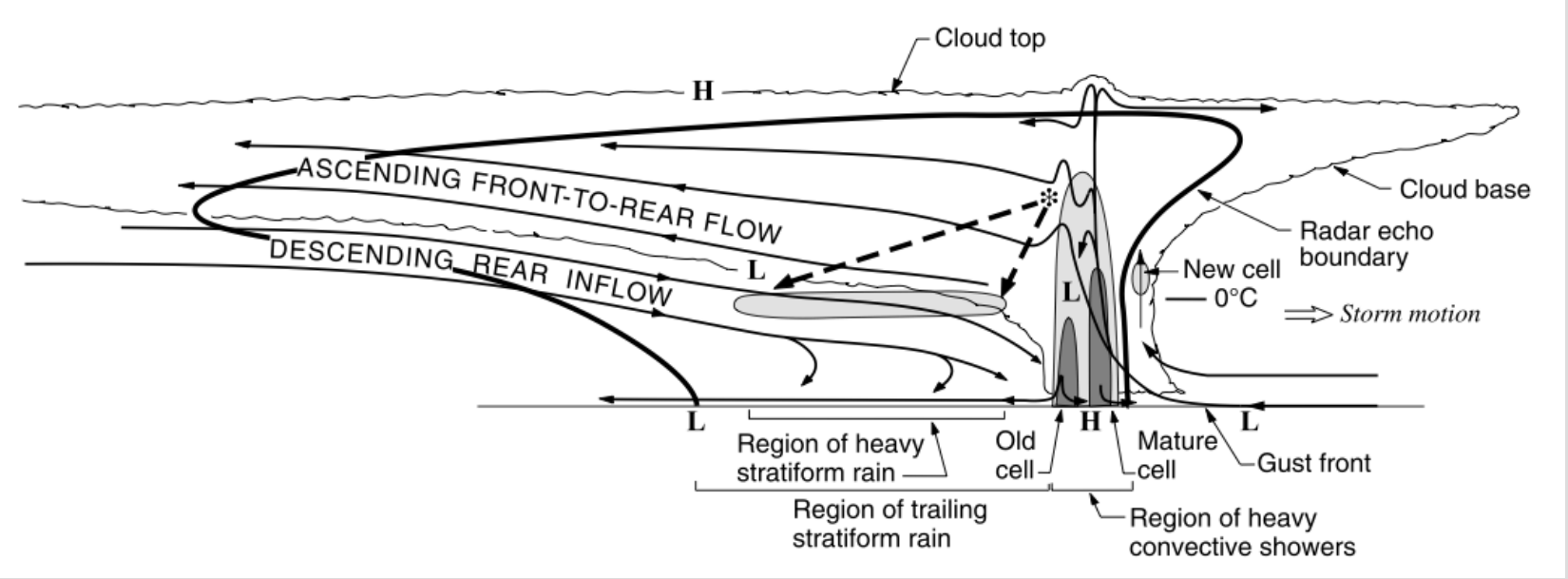

Houze (1993)

Generation of PV within a MCS
Heating = latent heat release by condensation
Cooling = evaporation of condensate

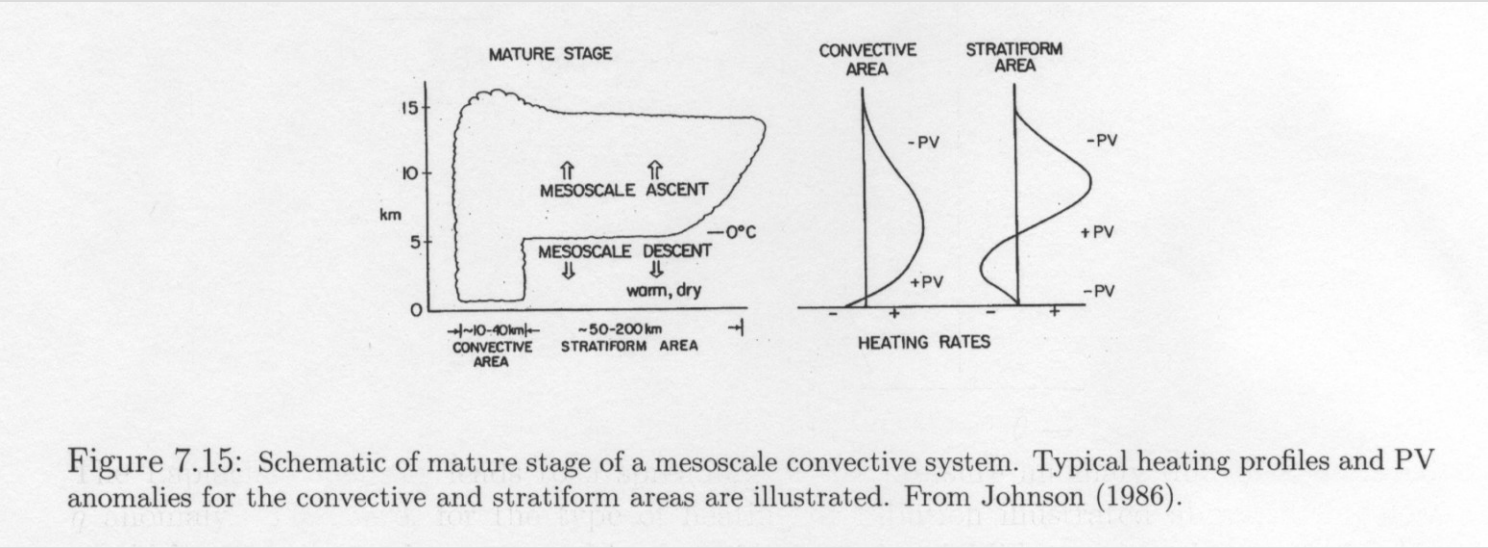

Figure 7.15: Schematic of mature stage of a mesoscale convective system. Typical heating profiles and PV anomalies for the convective and stratiform areas are illustrated. From Johnson (1986).

Convective core: Strong convective heating located in mid-troposphere. But PV anomalies above and below the heating are of too small of spatial scale to be geostrophically balanced and dissipate.

Stratiform area: Heating anomaly is shifted upward and cooling occurs in the lower troposphere due to evaporative cooling. Leads to generation of a +PV anomaly in the mid-troposphere that may be of sufficient scale to be geostrophically balanced and form a mesoscale convective vortex (MCV).

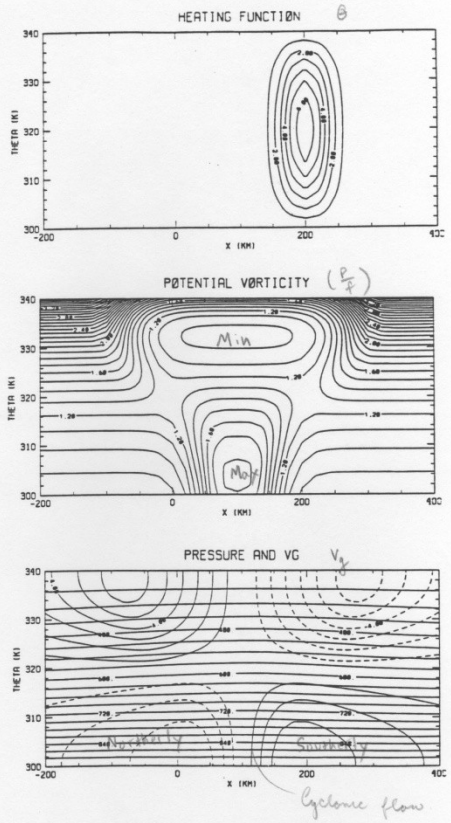

Fig. 11 (a) Heating function for the no stratiform case. For both model simulations, the squall line started at $X = 0$ and propagated to $X = 200$ km. Values are kelvins per hour with a contour interval of 1 K h^{-1}. (b) Dimensionless potential vorticity P/f in the wake of the squall line. Contour interval is 0.1. (c) Geostrophic flow along the squall line in meters per second with a contour interval of 1 m s^{-1}. Negative values represent northerly flow for a north-south aligned squall line. Also shown are isolines of pressure with a contour interval of 30 mb. From Hertenstein and Schubert (1991)

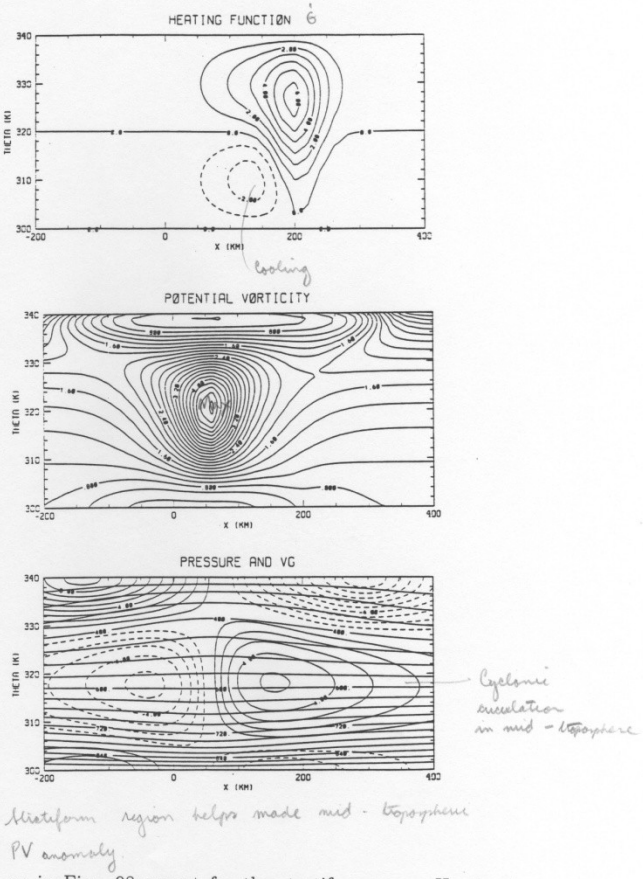

Fig. 12 Same as in Fig. 98 except for the stratiform case. Heating is indicated by solid contours while dashed lines represent coolings. Note that the contour interval for the potential vorticity field is 0.2. From Hertenstein and Schubert (1991)

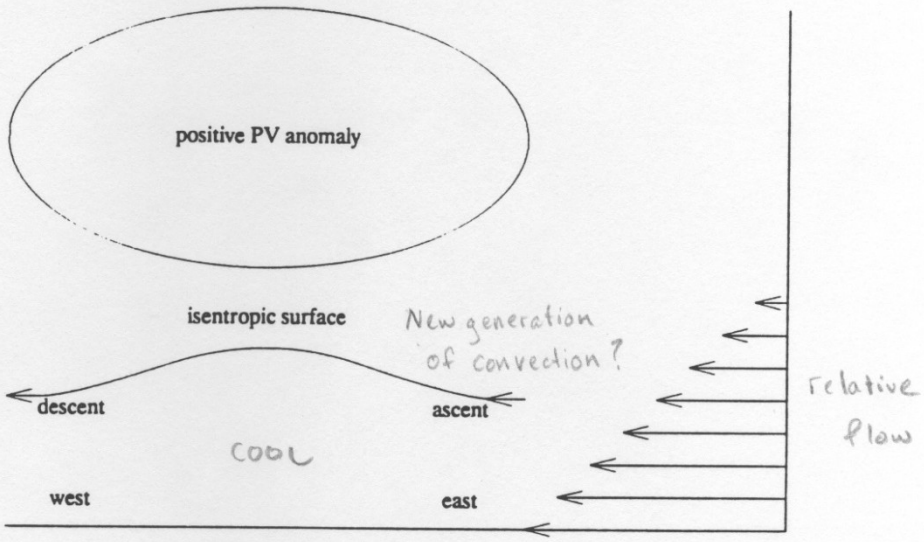

Fig. 13 Sketches of mechanism by which lifting might occur in the presence of a potential vorticity anomaly in shear. The ambient shear is confined to the east-west plane. Ambient shear is limited to below the potential vorticity anomaly here for clarity. In a frame in which the anomaly is stationary, the relative environmental wind causes flow on the perturbation isentropic surface caused by the potential vorticity anomaly. Ascent and descent occurs as illustrated. From Raymond and Jiang (1990)

Mesovortex formation with decay of MCS convection

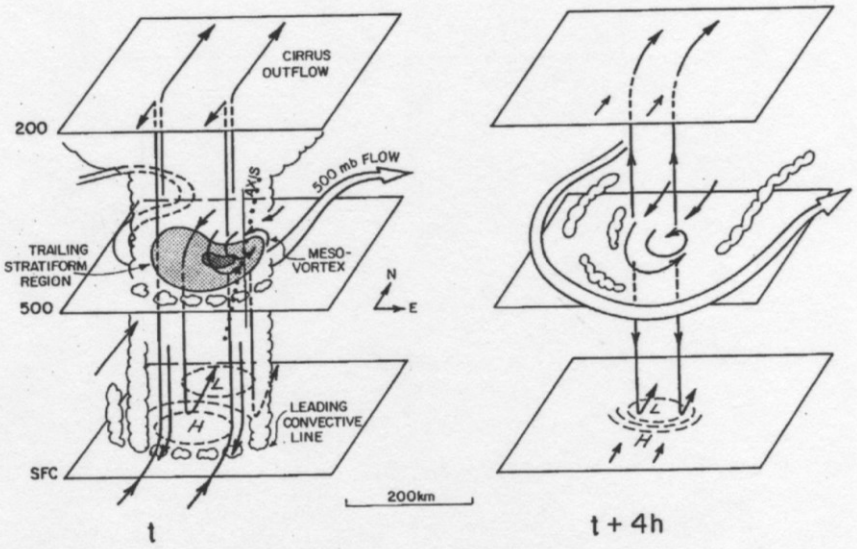

Figure 7.20: Idealized cloud and system-relative flow structure during decaying squall-line stage (t) and fully developed mesovortex stage ($t+$ 4 h). Solid arrows denote storm-relative flow, and open arrows large-scale 500-mb flow. Dotted line indicates approximate vertical extent and tilt (toward the northeast) of mesovortex core. From Johnson and Bartels (1992).

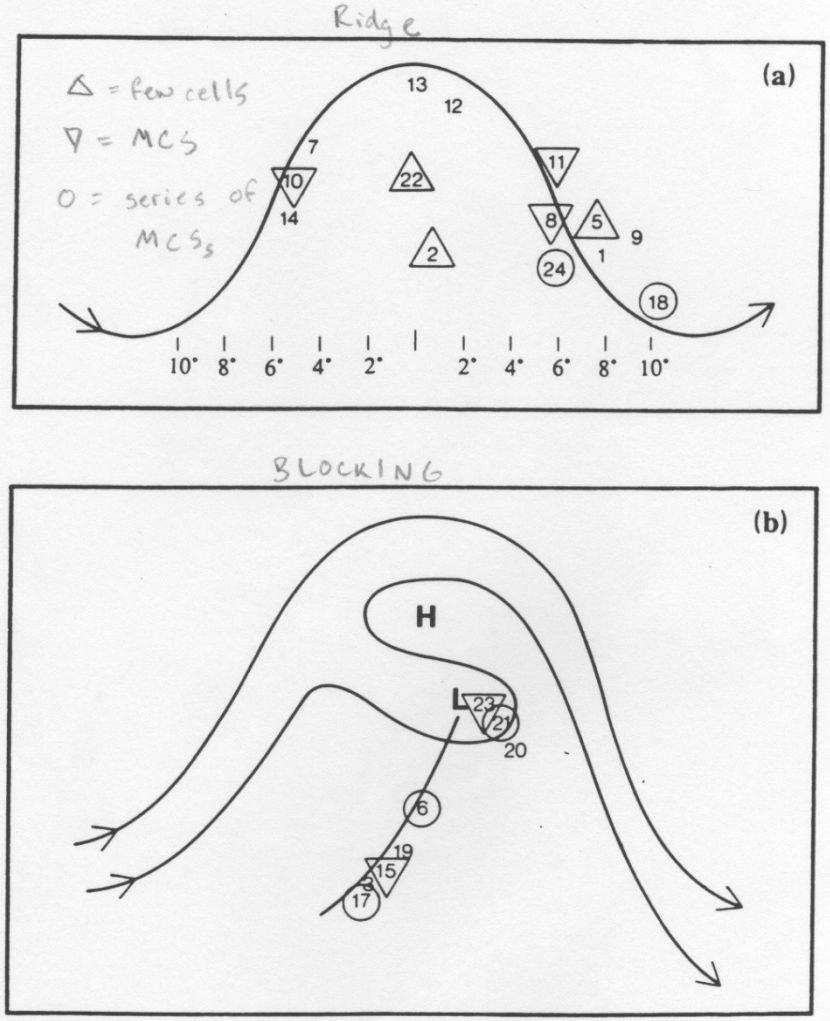

Fig. 9 Degree of subsequent activity associated with each MCV event is shown symbolically: case number alone indicates no activity, triangle = few cells, inverted triangle = MCS, and circles = a series event. (a) Location (expressed in degrees of longitude from ridge axis) of MCV events relative to 500-mb large-scale flow and ridge. Note an average scale of the ridge is 30° longitude. (b) Location of MCV events associated with a 500-mb blocking pattern. From Bartels and Maddox (1991)

Propagation and regeneration of MCS convection (Carbone et al. 2002, JAS)

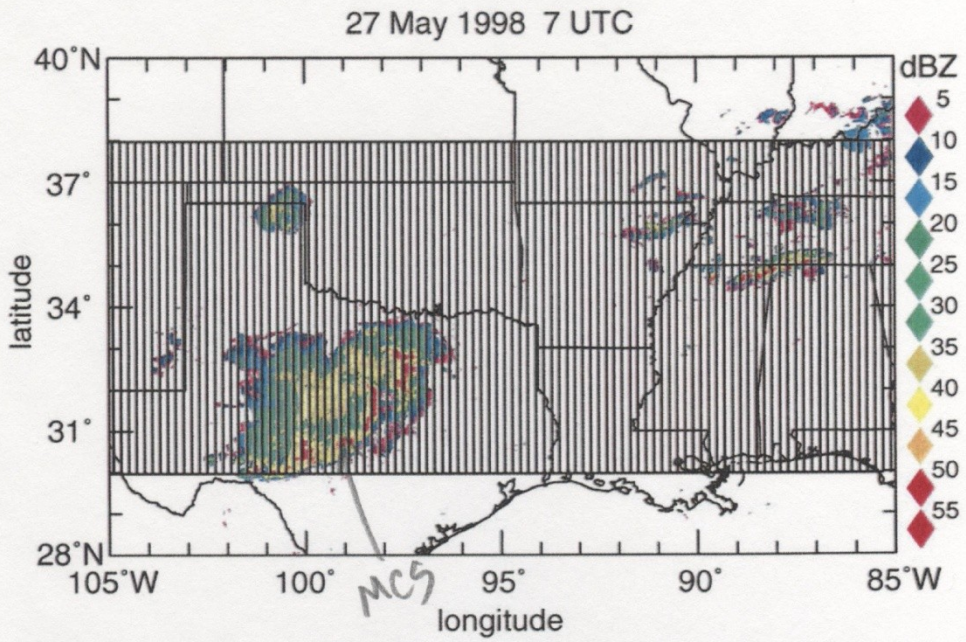

FIG. 9. Regional Hovmöller computational domain across southern tier of states. A leading-line, trailing stratiform mesoscale convective system is present at 0700 UTC 27 May 1998.

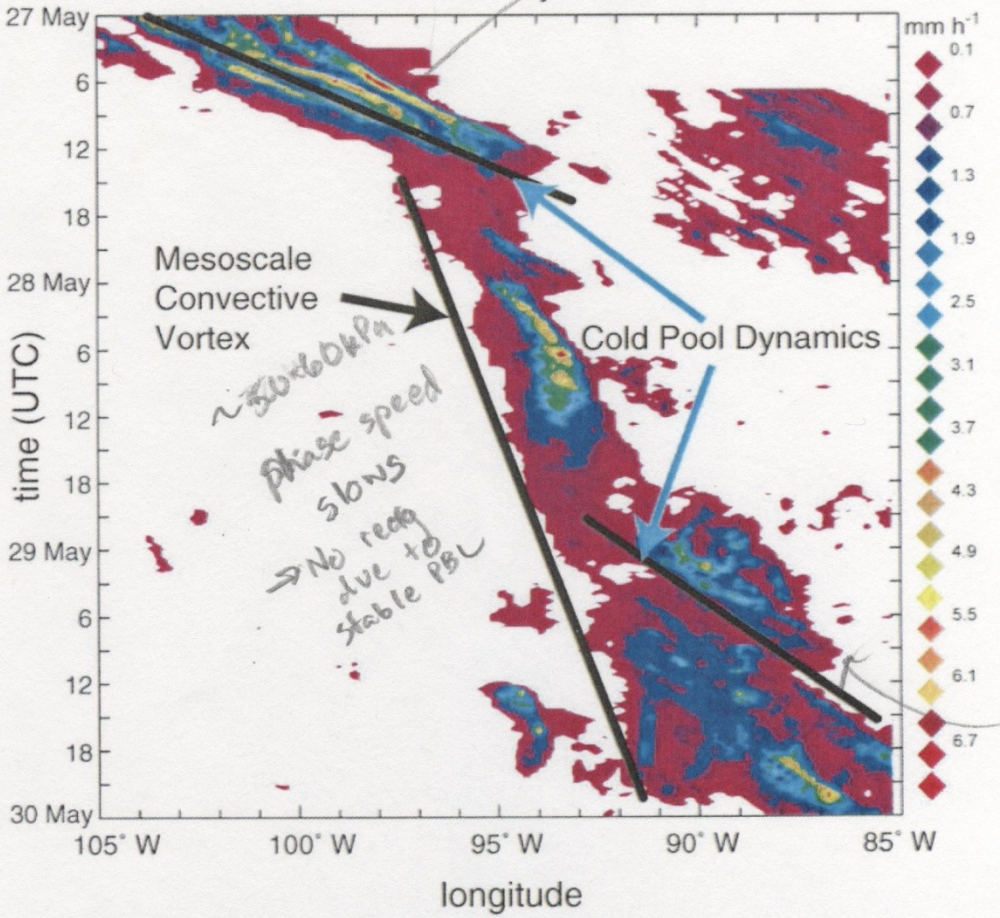

FIG. 10. Radar-derived rain-rate Hovmöller diagram for 27–29 May 1998 in the southern region. Note sudden changes in slope, coincident with (a) the MCS in Fig. 9, (b) precipitation associated with a convectively generated MCV, and (c) small squalls that are initiated within the MCV but rapidly propagate eastward from it.

East of 82°W there is an abrupt decrease in radar echo diurnal amplitude compared to the seasonal average and

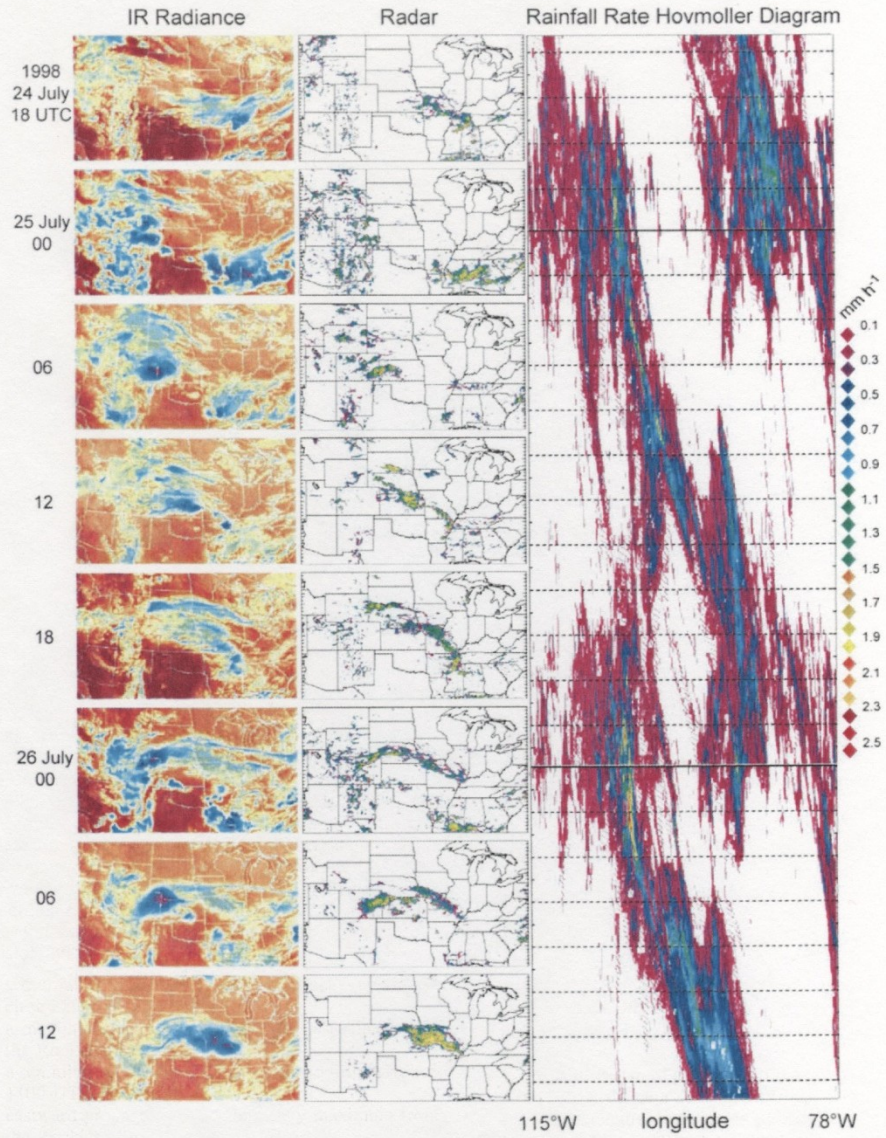

FIG. 11. Example of the "monsoon regime." Left column is sequence of enhanced GOES IR images over North America from (top) 1800 UTC 24 Jul 1998 through (bottom) 1200 UTC 26 Jul 1998. Center column is sequence of NOW*rad* images at the same times. Right column, matched in time to the GOES and radar images, is an expanded view of Fig. 6b for the period indicated. Note the consistent continent-scale coherent propagation.

For most MCS-generated convection in late summer in eastern 2/3 of the U.S., the ultimate generation point for theses systems is the diurnally-forced convection on the Rocky Mountains.

They then propagate east around the periphery of the monsoon ridge.

Ditto for organized monsoon convection in Arizona, except it propagates west.

MCS feedbacks to synoptic-scale and global scale

Impact on synoptic-scale flow: Generation of mesovortices and upper-air anticyclones

Convective transports of heat, momentum and moisture. Very important in tropics (as discussed in Liz Ritchie's class).

Upper-level cloud shields affect radiation budget

Affect tropopause structure and properties of the lower stratosphere (e.g. gravity waves associated with squall lines)

Horizontal and vertical transport of aerosols and chemical species.

MCS feedbacks to synoptic-scale and global scale

Impact on synoptic-scale flow: Generation of mesovortices and upper-air anticyclones

Convective transports of heat, momentum and moisture. Very important in tropics (as discussed in Liz Ritchie's class).

Upper-level cloud shields affect radiation budget

Affect tropopause structure and properties of the lower stratosphere (e.g. gravity waves associated with squall lines)

Horizontal and vertical transport of aerosols and chemical species.

GIVEN ALL THOSE REALLY IMPORTANT FEEDBACKS, THE BAD PART IS THAT YOU NEED A CONVECTIVE RESOLVING SCALE ON THE ORDER OF A KILOMETER GRIDSPACING. REPRESENT MCSs PROPERLY IN A FORECAST MODEL ☹